Graded photonic crystal terahertz quantum cascade lasers

Y. Chassagneux,[1] R. Colombelli,[1,a)] W. Maineult,[2] S. Barbieri,[2] S. P. Khanna,[3] E. H. Linfield,[3] and A. G. Davies[3]
[1]*Institut d'Electronique Fondamentale, Université Paris-Sud and CNRS, UMR8622, 91405 Orsay, France*
[2]*Laboratoire MPQ, Université Paris 7 and CNRS, UMR7162, 75013 Paris, France*
[3]*School of Electronic and Electrical Engineering, University of Leeds, Leeds LS2 9JT, United Kingdom*

(Received 23 October 2009; accepted 11 November 2009; published online 20 January 2010)

The use of integrated photonic structures to tailor the behavior of light is extremely promising for optimizing performance and for introducing advanced functionalities into optoelectronic devices. We demonstrate a powerful method based on photonic-band engineering which allows the optimization of the resonator quality factors of devices operating on band-edge photonic-crystal states. We also show that carefully designed π-shifts in two-dimensional photonic-resonators give enhanced beam properties. The application of these general techniques to terahertz quantum cascade lasers yields improved maximum operating temperatures, and angularly narrow, single-lobed surface emission of $\approx 12° \times 8°$. The devices operate at $\approx$2.8/2.9 THz, with peak output powers of 5 mW at 78 K. © *2010 American Institute of Physics*. [doi:10.1063/1.3273056]

Terahertz (THz) frequency quantum cascade (QC) lasers are compact semiconductor sources, which currently operate over the frequency range from 1.2 to 5 THz ($\lambda = 250-60$ μm).[1] They have promising applications for astronomy, imaging, and spectroscopy. The highest reported operating temperatures for THz QC lasers have been obtained using highly-confining double plasmon waveguides,[2] commonly called metal-metal waveguides. However, their extreme light confinement yields an emission pattern from the device end facet which suffers from a marked lack of directionality.[3] This lack of symmetric and low-divergence far fields is a critical issue for applications, thus explaining the attention paid recently by the international research community to "beam-shaping." For example, the emission patterns can be improved by attaching horn antennas onto the resonator facets,[4,5] by using microdisks/microrings with a radial grating acting as an out-coupler,[6] or by using third order distributed-feedback lasers.[7] Alternative strategies employ one-dimensional[8,9] or two-dimensional (2D) photonic crystal (PC) structures[10] and lead to surface emission, and to angularly narrow—but not single-lobed—output patterns.[11]

In this letter, we demonstrate a powerful and general method based on photonic-band engineering to optimize simultaneously the resonator in-plane quality factor ($Q_{\parallel}$) and thus the performance of PC (THz) lasers, and to achieve angularly narrow, single-lobed emission from the device top surface. Furthermore, the output is spectrally single-mode.

Figure 1(a) shows a schematic diagram of the device structure and its operation. The laser active core is sandwiched between two metallic plates as follows: the photonic-crystal, patterned on the top metallization, acts simultaneously as resonator and out-coupler for the cavity photons through a second order diffraction process. It is not necessary to etch into the semiconductor through the holes in the upper metal layer, greatly simplifying the processing. The QC laser structure (L207) is GaAs/AlGaAs-based with nominal emission centered at a frequency of 2.7 THz. Details of the growth and heterostructure design can be found in Ref. 11. Furthermore, as described in Ref. 10, Mur's absorbing boundary conditions can be, and have been here, experimentally implemented at the edge of the PC resonators, making use of the elevated absorption of the doped, semiconductor top contact layers.

The objective of our work is to devise a general strategy to improve the $Q_{\parallel}$-factor of PC band-edge devices, and to achieve an angularly narrow, single-lobed surface output far-field profile. Angularly narrow, single-lobed surface emission

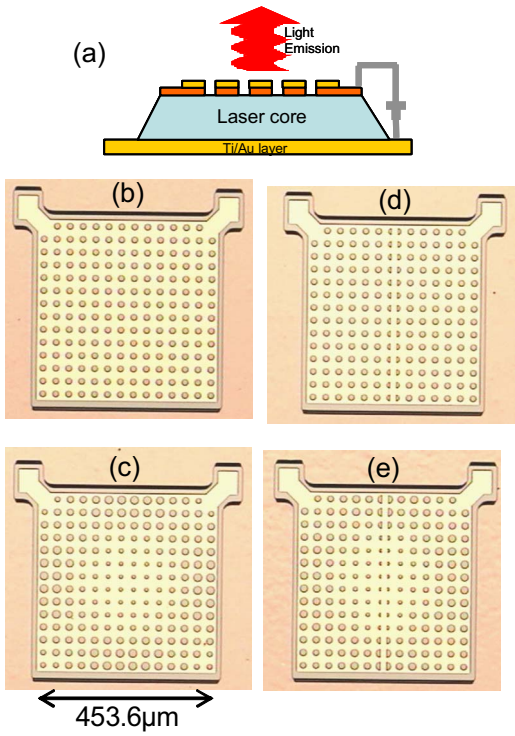

FIG. 1. (Color online) (a) Schematic structure of the device, and illustration of its operating principles. [(b)–(e)] Microscope images of the devices (top view). For all devices, the period of the PC is 32.4 μm. Small regions in two corners of each device are introduced for wire bonding. (b) Standard PC, the hole radius is 8.1 μm; (d) the same structure as (b) with a π-shift; [(c) and (e)] graded PC structures with optimized $Q_{\parallel}$-factors, with and without phase shift, respectively. The radii of the holes are in the range 5.4–10.8 μm.

a)Electronic mail: raffaele.colombelli@u-psud.fr.

can be obtained by introducing a π-shift phase-delay into the PC structure.[12,13] As the triangular photonic lattice of Ref. 10 does not easily permit this, we employed a square photonic lattice, which naturally suits the implementation of a π-shift.[14] The Q-factor optimization is instead inspired by a graded-lattice approach, in which the hole-radius is varied across the lattice[15]—a concept that was originally developed for PC microcavity modes, typically in the presence of a full photonic gap. We demonstrate here, however, its extension to lasers operating on low-group velocity states of the photonic structure, commonly called *band-edge* lasers; grading the PC structure then results in a "gentle" confinement of the electromagnetic field inside the PC resonator. One of the novelties of this work is that these advanced photonic-band engineering techniques are applied to active devices operating under electrical injection. The $Q_{\parallel}$-factor optimization then leads to a reduction in the device size, and therefore injected electrical power, which is critical for future development of THz QC lasers.

Figures 1(b)–1(e) show photographs (top surface) of four families of fabricated devices. Figures 1(b) and 1(c) show the standard device, with and without $Q_{\parallel}$-factor optimization, respectively. Figures 1(d) and 1(e) show devices with the π-shift inclusion, again with and without $Q_{\parallel}$-factor optimization. Traditionally, phase-shifts have been introduced by increasing/decreasing the distance between two holes by half a period.[8,13] We have modified this strategy in order to obtain improved single-lobed far-field emission; every hole on the central vertical line has been split into two parts, and then separated by half a photonic-lattice period [see Figs. 1(d) and 1(e)]. It can be shown, that a square-lattice PC device of this kind tends to lase on the monopolar band-edge state at the Γ-point of the photonic band structure, which has the highest Q-factor. Since the energy maxima are localized in the holes (monopolar mode), our design of the π-shift induces only a limited field perturbation over the whole structure. A bonding wire is needed for current injection. To avoid distortion to the device emission pattern (as observed in Ref. 10), small bonding pads are introduced at two mesa corners. These pads are very unlikely to lase as microcavities since absorbing boundary conditions have been left in place around them, and we have previously shown in Ref. 16 that microcavities of this kind are not functional.

Reducing the device surface area leads to a reduction of the operating current, which is in general favored for applications (reduced power consumption). The devices presented in this work have the same area as a 2 mm$\times$120 μm ridge waveguide (roughly 40% smaller than the devices presented in Ref. 11). Owing to the long wavelength of light in the THz frequency range, however, the small cross-sectional area leads to a reduced number of photonic-lattice periods. In the present work, only seven periods are incorporated from the center of the PC structure [see Figs. 1(b)–1(e)], Such a reduction in photonic-lattice periods lowers the device $Q_{\parallel}$-factor, leading to increased threshold current density (J_{th}) and reduced maximum operating temperature (T_{max}). The optimization of the PC resonator quality factor is thus clearly a crucial issue for device development.

It has been shown—for PC microcavity lasers operating with full photonic gaps—that grading the hole size across the PC can increase the Q-factor by creating a *photonic heterostructure*.[15] Our case is different, the lasers operate on band-edge states, and so the electromagnetic field is delocalized across the whole device surface. A distributed feedback mechanism—and not the presence of a photonic gap—is responsible for light confinement. However, we have found that grading the hole radius across the PC—as shown in Figs. 1(c) and 1(e)—leads to improved in-plane Q-factors. To confirm this, finite-difference time-domain (FDTD) 2D simulations were performed using the MEEP package developed at MIT (Ref. 17) (details of our simulation strategy can be found in Ref. 11). The calculated $Q_{\parallel}$-factors increase from 63.5 to 126.5 following optimization of the standard PC resonators [Figs. 1(b) and 1(c)]. When the π-shift is introduced, the values are slightly reduced, but an increase from 53.3 to 113.6 is still seen using the graded PC [Figs. 1(d) and 1(e)]. In both cases, therefore, grading the PC doubles the $Q_{\parallel}$-factor.

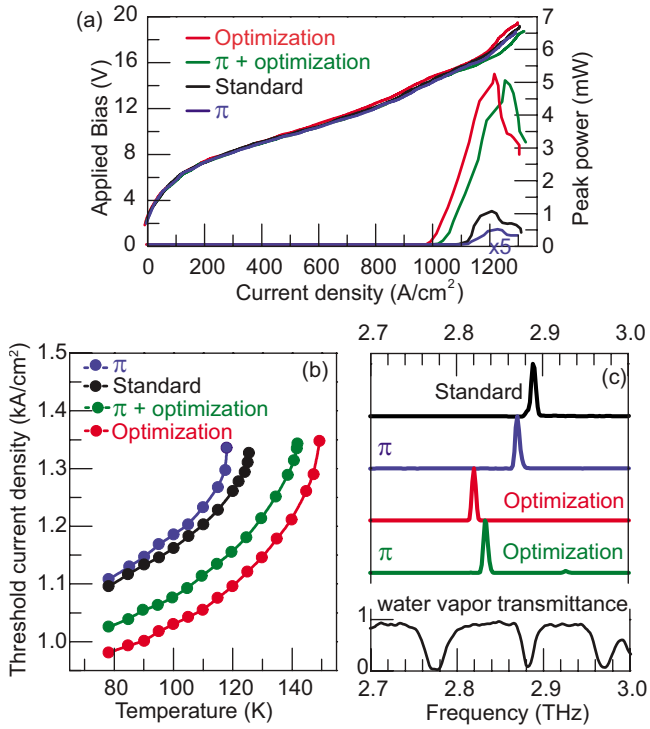

FIG. 2. (Color online) Electro-optical characteristics of the lasers. (a) characteristics voltage-light-current density (LJV) of devices with and without π-shift, and with and without Q-factor optimization. The measurements were performed at 78 K, using a Peltier-cooled far-IR DTGS detector. The devices were operated at a 20 kHz repetition rate, with 300 ns wide pulses. (b) Temperature dependence of J_{th} for the four devices; (c) Typical laser spectra of the devices. The devices without optimization lase on a water vapor absorption line, which could partially explain the lower measured output power.

The QC lasers were mounted in a cryostat for electro-optical characterizations. Figure 2(a) shows the light-current-voltage characteristics of devices with and without Q-factor optimization, and with and without π-shift. Optimized devices (green and red curves) exhibit a lower threshold current density, and higher output peak power of $\approx$5 mW under pulsed operation at 78 K. Although the power measurements were performed while purging with dry nitrogen gas, we cannot attribute the output increase to the optimization procedure unambiguously. In fact, the emission frequency of nonoptimized devices falls almost exactly onto a water vapor absorption line [Fig. 2(c)]. However, the measured T_{max} are consistent with the threshold current density data, and in par-

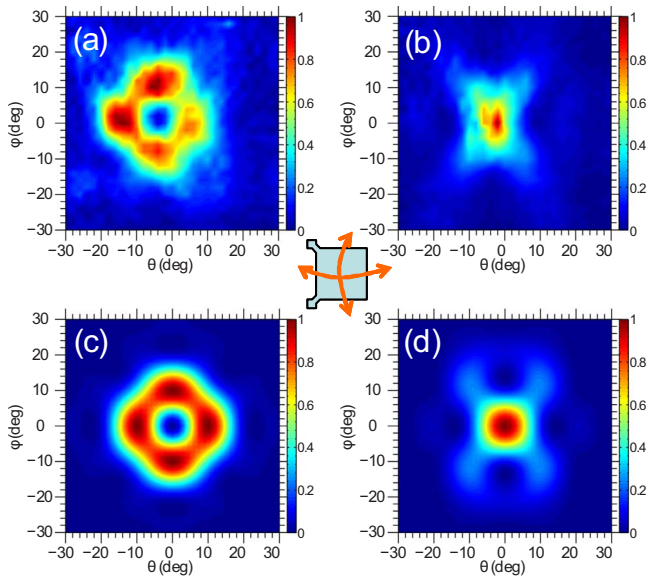

FIG. 3. (Color online) Far-field emission patterns of the lasers. The central inset defines the angles of scanning. A Golay cell detector was used for the measurement. [(a) and (b)] correspond to the measured far-field patterns of the optimized structures, without and with the π-shift phase-delay, respectively [Figs. 2(c) and 2(e)]. [(c) and (d)] Show the corresponding predicted far-fields, respectively.

ticular follow exactly the calculated trend expected for the different $Q_{\parallel}$-factors. It can be observed that the optimization procedure increases T_{max} by 25 K, from 124 to 149 K, for PC lasers without π-shift, and from 117 to 142 K with π-shift [Fig. 2(b)]. The emission spectra are single mode for all injected currents except for the structure with a π-shift and optimization, which presents a very small deviation from a pure monomode behavior [Fig. 2(c)].

The far-field emission patterns of the devices with $Q_{\parallel}$-factor optimization were measured by scanning a Golay cell detector at constant distance from the lasers. (The scanning angles are defined in the central inset of Fig. 3). In the absence of a phase-shift [Fig. 3(a)] a four-lobe far-field pattern is obtained, with a doughnut-like shape as is expected for PC lasers operating on band-edge states. The introduction of a π-shift [Fig. 3(b)] yields a clear single-lobed far-field pattern instead, with an angular full-width-at-half-maximum cone of $12° \times 8°$. The almost diffraction-limited angular spreading confirms that the electromagnetic field of the lasing mode is delocalized over the whole PC. The same 2D FDTD simulations, which allow us to estimate the $Q_{\parallel}$-factor, also give the predicted far-field patterns, with the near-to-far-field conversion being performed using only the transverse electromagnetic fields in the holes. This procedure is justified because, at THz frequencies, the metallic PC lets energy flow out from the holes only. The predicted far-fields [Figs. 3(c) and 3(d)] are in excellent agreement with the experiment, even for the weaker features.

In order to quantify the quality of the output beam, we employ a figure of merit recently used for mid-IR QC lasers,[18] and frequently used for antennas the directivity, defined as $D=10\times\log_{10}(2\pi\ I_{peak}/I_{total})$. It is the ratio of the peak intensity (I_{peak} in Watts per steradian) in the far-field to the total emission power (I_{tot} in Watts) into half space. We obtain a directivity D=16.5 dB for the optimized structure without phase-shift, and D=19.5 dB with phase-shift. For comparison a single-plasmon THz QC laser in ridge geometry typically exhibits a directivity of 14 dB,[3] while mid-infrared QCLs with plasmonic collimators[18] yield a directivity of 26.9 dB.

The device design presented here stems from a trade-off between two requirements: on the one hand, angularly narrow beam-shapes, and reasonable output powers, in general require the mode to be delocalized over the photonic structure. This is the reason for operating over band-edge states with low group-velocity. On the other hand, an improved $Q_{\parallel}$-factor is favored by spatially localized PC modes, which are characterized by reduced power out-flow at the device boundaries. Even in the absence of a photonic-gap, a graded structure can still strongly increase the Q-factor by inducing a gentle, smooth spatial confinement of the electromagnetic field in the resonator.

In summary, photonic-band engineering is a very powerful procedure for optimizing quality factors and, simultaneously, radiation patterns of PC lasers, even under electrical injection. Application to semiconductor THz lasers yields optimized performance and single-lobed, surface emission with high directivity. The design strategy is general, opening up opportunities also in other regions of the electromagnetic spectrum.

We thank François Julien, Jean-Michel Lourtioz, and Carlo Sirtori for useful discussions. The device fabrication was performed at the nanocenter CTU-IEF-Minerve. This work was conducted as part of a EURYI scheme award (www.esf.org/euryi). S.P.K., E.H.L., and A.G.D. acknowledge support from the EPSRC (U.K.) and the EC project *NOTES*. SB acknowledges partial financial support from the DGA, and the C-Nano Ile-de-France.

[1] B. S. Williams, Nat. Photonics **1**, 517 (2007).
[2] S. Kumar, Q. Hu, and J. L. Reno, Appl. Phys. Lett. **94**, 131105 (2009).
[3] P. Gellie, W. Maineult, A. Andronico, G. Leo, C. Sirtori, S. Barbieri, Y. Chassagneux, J. R. Coudevylle, R. Colombelli, S. P. Khanna, E. H. Linfield, and A. G. Davies, J. Appl. Phys. **104**, 124513 (2008).
[4] W. Maineult, P. Gellie, A. Andronico, P. Filloux, G. Leo, C. Sirtori, S. Barbieri, E. Peytavit, T. Akalin, J.-F. Lampin, H. E. Beere, and D. A. Ritchie, Appl. Phys. Lett. **93**, 183508 (2008).
[5] M. I. Amanti, M. Fischer, C. Walther, G. Scalari, and J. Faist, Electron. Lett. **43**, 573 (2007).
[6] E. Mujagić, C. Deutsch, H. Detz, P. Klang, M. Nobile, A. M. Andrews, W. Schrenk, K. Unterrainer, and G. Strasser, Appl. Phys. Lett. **95**, 011120 (2009).
[7] M. I. Amanti, M. Fischer, G. Scalari, M. Beck, and J. Faist, Nat. Photonics **3**, 586 (2009).
[8] S. Kumar, B. S. Williams, Q. Qin, A. W. M. Lee, and Q. Hu, Opt. Express **15**, 113 (2007).
[9] J. A. Fan, M. Belkin, F. Capasso, S. Khanna, M. Lachab, A. G. Davies, and E. H. Linfield, Opt. Express **14**, 11672 (2006).
[10] Y. Chassagneux, R. Colombelli, W. Maineult, S. Barbieri, H. E. Beere, D. A. Ritchie, S. P. Khanna, E. H. Linfield, and A. G. Davies, Nature (London) **457**, 174 (2009).
[11] Y. Chassagneux, R. Colombelli, W. Maineult, S. Barbieri, S. P. Khanna, E. H. Linfield, and A. G. Davies, Opt. Express **17**, 9491 (2009).
[12] S. Li, G. Witjaksono, S. Macomber, and D. Botez, IEEE J. Sel. Top. Quantum Electron. **9**, 1153 (2003).
[13] E. Miyai and S. Noda, Appl. Phys. Lett. **86**, 111113 (2005).
[14] G. Witjaksono, S. Li, J. J. Lee, D. Botez, and W. K. Chan, Appl. Phys. Lett. **83**, 5365 (2003).
[15] K. Srinivasan, P. E. Barclay, O. J. Painter, J. Chen, A. Y. Cho, and C. Gmachl, Appl. Phys. Lett. **83**, 1915 (2003).
[16] Y. Chassagneux, J. Palomo, R. Colombelli, S. Dhillon, C. Sirtori, H. Beere, J. Alton, and D. Ritchie, Appl. Phys. Lett. **90**, 091113 (2007).
[17] A. Farjadpour, D. Roundy, A. Rodriguez, M. Ibanescu, P. Bermel, J. P. Joannopoulos, S. G. Johnson, and G. Burr, Opt. Lett. **31**, 2972 (2006).
[18] N. Yu, R. Blanchard, J. Fan, Q. Wang, C. Pflügl, L. Diehl, T. Edamura, M. Yamanishi, H. Kan, and F. Capasso, Opt. Express **16**, 19447 (2008).